

## Trifluoroacetate-bonded polyethylene graphene oxide composite as a novel and efficient catalyst for the synthesis of benzimidazoles under solvent-free conditions

Esmael Rostami,\* Seyed Mahdi Haghayeghi

Department of chemistry, Payame Noor University, PO BOX 19395-3697 Tehran, Iran.

Received 2 May 2020; received in revised form 5 January 2021; accepted 10 January 2021

### ABSTRACT

A green and efficient trifluoroacetate-bonded polyethylene graphene oxide composite was utilized in this research to prepare benzimidazoles with good to excellent yield under a solvent-free condition. The trifluoroacetate-bonded polyethylene graphene oxide composite was constructed by polyethylene/diethylenetriamine-functionalized graphene oxide composite bonded by 2-aminothiazole and  $\text{CF}_3\text{COOH}$  moieties. Fourier transform infrared (FTIR) spectroscopy, X-ray diffraction (XRD) analysis, field emission scanning electron microscopy (FESEM), energy dispersive x-ray spectroscopy (EDS), and thermogravimetric analysis (TGA) were also employed to characterize the composite. Benzimidazoles were synthesized by reacting 1,2-phenylenediamine with aromatic aldehydes in the presence of composite (0.02 g) under solvent-free conditions at  $75^\circ\text{C}$ . The composite was recovered and used in five runs without considerable loss of activity. Compared to the other catalysts employed for the synthesis of benzimidazole, the present composite (catalyst) benefits from a series of advantages such as cost-effectiveness, easy storage and handling, recoverability and durability, environmental friendliness, non-metallic nature, and ease of disposal. The present synthetic route has also some advantages, including, moderate condition, easy workup, solvent-free nature, and environmental safety.

**Keywords:** Polyethylene composite, graphene oxide, trifluoroacetic acid catalyst, benzimidazole, solvent-free.

### 1. Introduction

In recent years, organic chemists have developed green protocols for the synthesis of organic compounds [1]. These protocols use heterogeneous catalysts and no solvent to offer environmentally-benign and sustainable processes [2]. In the design of green processes, the reaction media are a key factor since the industrial-scaled toxic organic solvents can pose serious hazards to the environment. In this regard, the elimination of such toxic compounds and the use of solvent-free conditions can contribute highly to protecting the ecosystems [3].

Among the heterogeneous catalysts, carbon-containing catalysts such as graphene and graphene oxide are one of the most promising candidates [4]. Polymer-functionalized graphene compounds have found diverse applications (including catalysis) [5]. Among the industrial polymers, polyethylene has been employed

for several applications [6]. The use of functionalized-polyethylene in the synthesis of composites and nanocomposites can open new applications for polyethylene while reducing the wastes [7].

Benzimidazole is a nitrogen-containing heterocyclic compound [8] which is present in a large number of drugs and biologically active molecules [9]. This synthon and its derivatives have been widely employed in the design and synthesis of new biologically active species [10]. Benzimidazole derivatives have also shown promising therapeutic properties including anti-inflammatory [11], anthelmintic [12], antifungals [13], antiviral [14], analgesic [15], anticancer [16], antiulcer [17], antibacterial [18] and antihypertensive [19] activities.

Due to its importance, the synthesis of benzimidazoles has been widely explored. Several common processes have been proposed for their synthesis using 1,2-phenylenediamine and carboxylic acids, aldehydes or acid halides in organic solvents in the presence of toxic and homogeneous catalysts [20]. Moreover, numerous

\*Corresponding author:

E-mail address: [Esmaelrostami@gmail.com](mailto:Esmaelrostami@gmail.com);  
[e.rostami@pnu.ac.ir](mailto:e.rostami@pnu.ac.ir) (E. Rostami)

procedures have been reported which mainly include the reaction of ortho phenylenediamine with aldehydes using catalysts such as, solid  $\text{Co}(\text{OH})_2$  and  $\text{CoO}$  (II) [21], indium triflate [ $\text{In}(\text{OTf})_3$ ] [22], polyphosphoric acid (PPA) [23], polyaniline-sulfate salt [24], heteropoly acids (HPAs) [25], alumina, silica gel, and zeolite HY [26], zinc triflate [27], lanthanum chloride [28], L-proline [29], silica sulfuric acid [30], ionic liquids [31],  $\text{Sm}(\text{OTf})_3$  [32], thiamine hydrochloride [33], sodium metabisulfite [34], ammonium acetate [35],  $\text{BF}_3 \cdot \text{Et}_2\text{O}$  [36], magnetic core-shell nanocomposite [37], and graphene oxide [38]. Most of the mentioned procedures suffer from harsh reaction conditions, toxic materials, expensive catalysts, high-temperature requirement, and low yields. In this regard, the development of a new environmentally-benign condition with excellent yields and simple workup can be helpful in the preparation of these valuable products. In this research, a novel PE@GO-DETA-Thiazole.TFA nanocomposite was successfully employed as a catalyst to synthesize benzimidazoles under solvent-free conditions.

## 2. Experimental

### 2.1. Materials and instrumentation

Reagents and solvents were supplied from Aldrich and Merck companies. Polyethylene functionalized with maleic anhydride was prepared according to the procedure reported in the literature [39-41]. The  $^1\text{H}$  and  $^{13}\text{C}$  NMR spectra were recorded by Bruker Avance 400 and 500 MHz spectrometers using  $\text{DMSO-d}_6$  as the deuterated solvent and TMS as an internal standard. Fourier Transform Infrared (FT-IR) spectra were measured using JASCO, FT/IR-6300 FT-IR spectrometer utilizing KBr pellets. Mass spectra were measured by Agilent model 5975c-inert MSD consisting of a Triple-Axis detector mass spectrometer. Bruker AXSD 8 Advance X-ray diffractometer was also utilized to record X-ray diffraction analysis (XRD) of powders using monochromatic  $\text{CuK}\alpha$ , radiation ( $\lambda=1.5406 \text{ \AA}$ ). Data were collected in the range of  $5\text{-}80^\circ$  at a scan rate of  $0.1^\circ \text{ min}^{-1}$ . IMECO 34 kHz frequency, 500W sonicate, was used to homogenize dispersed solutions. Stuart Scientific melting point apparatus was utilized to determine melting points. Morphologies and Energy Dispersive Spectroscopy (EDS) of samples were studied using TE-SCAN Field Emission Scanning Electron Microscope (FESEM). SDT Q600 V20.9 Build 20 apparatus was utilized to perform Thermogravimetric analysis (TGA) under Ar atmosphere.

### 2.2. Preparation of diethylenetriamine-functionalized graphene oxide (GO@DETA)

Modified Hummers method was utilized for the preparation of graphene oxide (GO) [42,43]. The mixture of graphene oxide (1g) and dimethylformamide (DMF, 30 mL) was sonicated for 30 min at room temperature. Then, DCC (0.6 g) and trimethylamine (0.75 mL) were added to the mixture and the reaction was continued for 48h. Finally, the mixture was diluted by water (5 ml) and DMF (30 mL), heated, hot filtered, and washed with hot ethanol (30 ml), hot deionized water (20 ml), and acetone (30 ml) followed by drying at room temperature to obtain fine black powders of GO@DETA. FT-IR (KBr): 612, 793, 1083, 1096, 1455, 1531, 1636, 2070, 2856, 2925,  $3438 \text{ cm}^{-1}$ .

### 2.3. Preparation of trifluoroacetate-bonded polyethylene graphene oxide composite (PE@GO-DETA-Thiazole-TFA)

The mixture of GO@DETA (0.1 g) and p-xylene (10 ml) was homogenized in an ultrasonic bath for 30 min at room temperature. In another flask, p-xylene (10 ml) was added to the polyethylene-functionalized maleic anhydride [39-41] and the mixture was homogenized by an ultrasonic bath for 30 min at  $60^\circ\text{C}$  followed by refluxing to dissolve the polymer. Then, GO@DETA solution was added and the mixture was heated and refluxed overnight. The stirring was then stopped and hexamethylenediisocyanate (HDMI, 0.2 ml) and trimethylamine (0.5 ml) were charged and kept at reflux for 4h. Consequently, 2-aminothiazole (0.2 g) was added. After 5 hours of refluxing, methanol (2 ml) was charged and the mixture was heated for another 2h under reflux conditions. Ultimately, water (5 ml) was added and the solution was purified by centrifugation followed by washing with hot ethanol twice, deionized water, and acetone and drying at room temperature and reduced pressure to reach PE@GO-DETA-Thiazole composite. To prepare the catalyst, 1,2-dichloroethane (15 ml) was added to PE@GO-DETA-Thiazole composite (0.5 g) and dispersed in an ultrasonic bath at  $60^\circ\text{C}$ . After cooling, trifluoroacetic acid (TFA, 0.3 ml) was added and stirred for 5h. Finally, the crude product was purified by centrifugation and washed with dichloromethane (5 ml) followed by drying at room temperature and reduced pressure to obtain PE@GO-DETA-Thiazole-TFA composite. FTIR (KBr): 717, 1037, 1081, 1203, 1247, 1326, 1396, 1463, 1515, 1567, 1619, 1675, 2844, 2915,  $3386 \text{ cm}^{-1}$ .

### 2.4. Synthesis of 4-[4-(4-bromophenyl)-3-aza-2-oxo-propyloxy] benzaldehyde (3)

4-hydroxy benzaldehyde (**2**, 1mmol, 0.122g) and  $\text{K}_2\text{CO}_3$  (1mmol, 0.14g) were added to N-(4-bromoaniline) - 2-chloroacetamide (**1** [44], 1mmol, 0.247g) in acetonitrile (25 mL) and refluxed for 48 h. The thin-layer

chromatography (TLC) was utilized to monitor the process. After cooling, water was added (50 mL) to the mixture and it was filtered. The crude precipitate was recrystallized in ethanol to obtain **3** with yield of 94% and the melting point of 153-154 °C.  $^1\text{H}$  NMR (500 MHz, DMSO- $d_6$ )  $\delta$ : 4.87 (s, 2H), 7.19 (d,  $J = 8.5$  Hz, 2H), 7.52 (d,  $J = 8.5$  Hz, 2H), 7.62 (d,  $J = 8.5$  Hz, 2H), 7.90 (d,  $J = 8.5$  Hz, 2H), 9.88 (s, 1H), 10.34 (s, 1H) ppm;  $^{13}\text{C}$  NMR (125 MHz, DMSO- $d_6$ )  $\delta$ : 190.79, 165.53, 162.15, 137.17, 131.20, 131.05, 129.59, 121.04, 114.85, 114.64, 66.50 ppm; MS (EI):  $m/z$  333 (M) $^+$ .

### 2.5. General procedure for the synthesis of benzimidazole derivatives

PE@GO-DETA-Thiazole-TFA composite (0.02 g) was added to 1,2-phenylene diamine (**7**, 1 mmol) and aldehyde (1 mmol). After mixing, the reaction was heated at 75 °C. The reaction time is reported in Table 1. Thin-layer chromatography (TLC) was employed to monitor the process. After adding of ethanol (5 ml) and hot filtering, the composite was finally collected on the filter paper. The filtrates were then purified by recrystallization in ethyl alcohol to afford the pure products.

### 2-[4-(4-nitrobenzyloxy) phenyl]-1H-benzimidazole (**6m**):

$^1\text{H}$  NMR (400 MHz, DMSO- $d_6$ )  $\delta$ : 5.25 (s, 2H), 6.97-7.03 (m, 2H), 7.28 (d,  $J=12\text{Hz}$ , 1H), 7.36 (d,  $J=12\text{Hz}$ , 1H), 7.51 (d,  $J=12\text{Hz}$ , 1H), 7.69-7.73 (m, 2H), 7.77-7.81 (m, 2H), 8.19 (d,  $J=8\text{Hz}$ , 1H), 8.26-8.34 (m, 3H) ppm;

$^{13}\text{C}$  NMR (100 MHz, DMSO- $d_6$ )  $\delta$ : 160.64, 158.32, 150.95, 148.01, 145.80, 145.45, 138.80, 131.94, 130.04, 129.69, 129.27, 129.13, 129.10, 128.71, 126.47, 124.83, 124.60, 124.52, 124.38, 124.27, 116.62, 116.29, 116.06, 115.25, 112.67, 68.95 ppm.

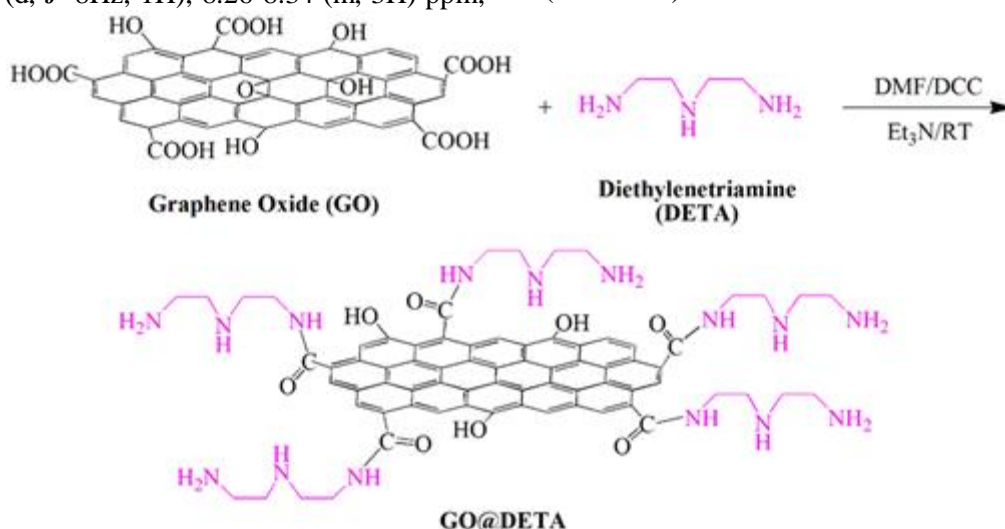
### 2-[4-(3-(4-Bromophenyl)-3-aza-2-oxopropoxy) phenyl]-1H-benzimidazole (**6n**)

$^1\text{H}$  NMR (500 MHz, DMSO- $d_6$ )  $\delta$ : 4.92 (s, 2H), 7.12-7.79 (m, 11H), 8.19 (d,  $J = 9$  Hz, 2H), 10.38 (s, 1H) ppm;  $^{13}\text{C}$  NMR (125 MHz, DMSO- $d_6$ )  $\delta$ : 165.60, 160.83, 148.82, 144.67, 137.22, 132.50, 132.41, 131.06, 130.99, 129.05, 127.66, 124.96, 124.56, 121.02, 115.25, 114.85, 114.45, 113.72, 113.46, 66.48 ppm; MS (EI):  $m/z$  422 (M) $^+$ .

## 3. Result and Discussion

### 3.1. Synthesis of graphene oxide, diethylenetriamine-functionalized graphene oxide

Modified Hummers method was employed to prepare graphene oxide (GO) [42, 43]. In the purification process, the reaction solvent was eliminated by adding deionized water and ultrasonic treatment to obtain nanostructured graphene oxide. Diethylenetriamine-functionalized graphene oxide (GO@DETA) was synthesized by reacting graphene oxide with diethylenetriamine (DETA) where dicyclohexylcarbodiimide (DCC) served as the coupling agent. DCC formed bonds between carboxylic acids of graphene oxide and diethylenetriamine (**Scheme 1**).



**Scheme 1.** Preparation of graphene oxide functionalized diethylenetriamine (GO@DETA).

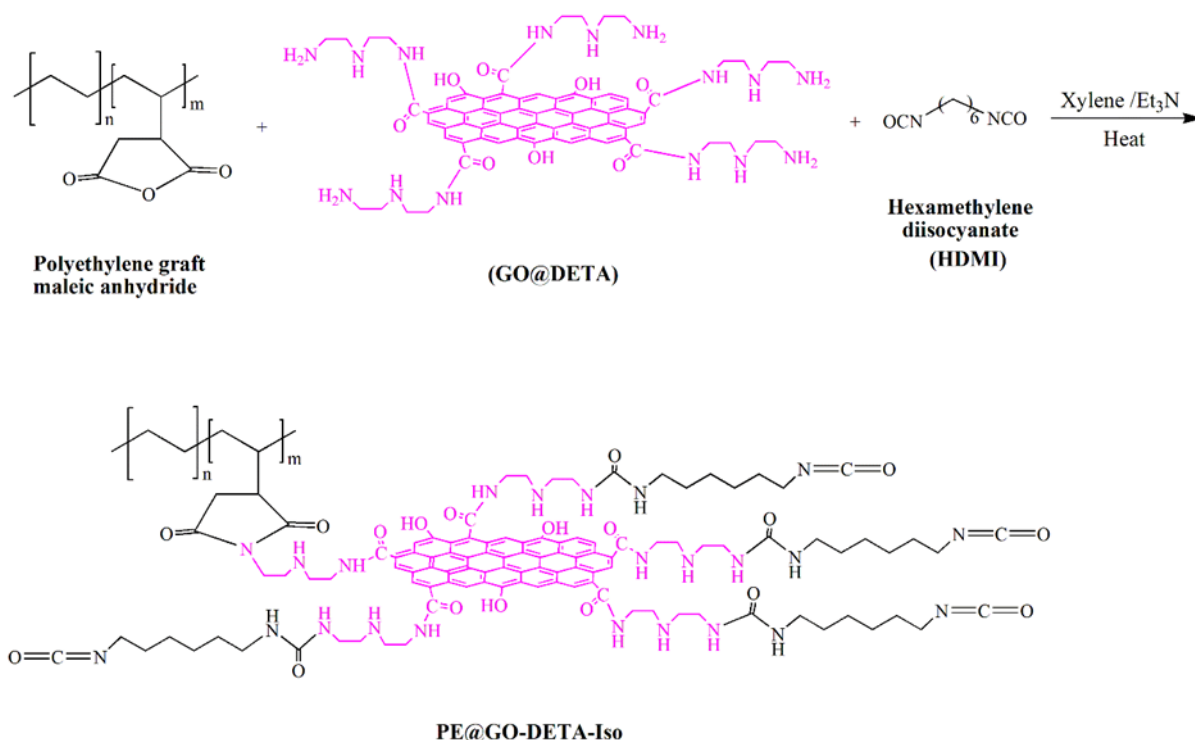
### 3.2. Synthesis of trifluoroacetate-bonded polyethylene graphene oxide composite

Polyethylene-factionalized maleic anhydride [39-41] can be readily reacted with amines [45,46]. Through this

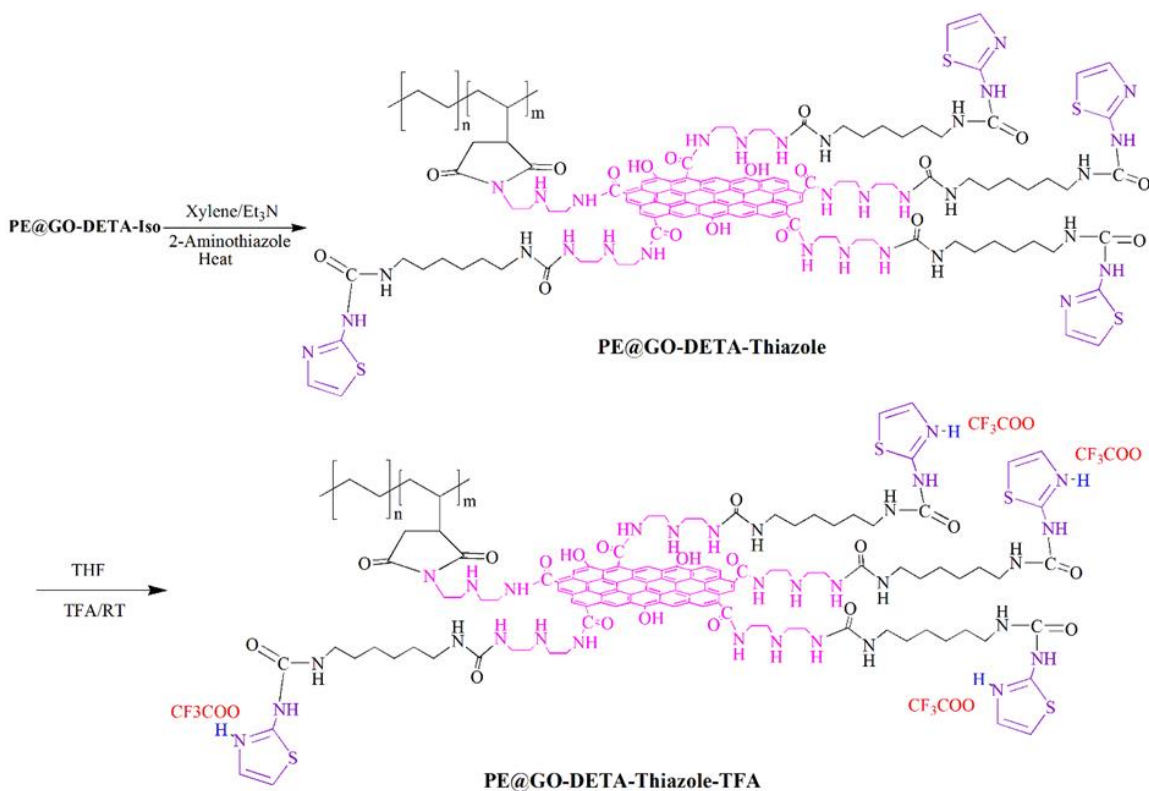
reaction, polyethylene and amine-functionalized graphene composite can be successfully prepared (**Schemes 2** and **3**). The composite was first prepared from the reaction of polyethylene-functionalized maleic anhydride and GO@DETA (**Scheme 2**). Then,

hexamethylenediisocyanate was added to the mixture and the reaction was continued to functionalize the graphene (**Scheme 2**). Subsequently, 2-aminothiazole was added to functionalize isocyanate to anchor the functional groups via urea formation (Scheme 3). Finally, methanol was added to remove the unreacted

isocyanate groups. Afterward, the resulting composite was dried under reduced pressure followed by treatment with trifluoroacetic acid to prepare the PE@GO-DETA-Thiazole-TFA composite (**Scheme 3**). The resulting composite was dried under reduced pressure and stored in a tight vial.



**Scheme 2.** Preparation of polyethylene and functionalized graphene oxide composite.



**Scheme 3.** Preparation of PE@GO-DETA- Thiazole-TFA composite.**3.3. FT-IR spectra**

FT-IR spectroscopy was utilized to confirm the synthesis of graphene oxide, Diethylenetriamine-functionalized graphene oxide (GO@DETA), and PE@GO-DETA-Thiazole-TFA composite (**Fig. 1**). Graphene oxide naturally contains carboxylic acid, ether, epoxide, hydroxyl, single and double bonds, and ketone functional groups. **Fig. 1a** shows the FTIR spectrum of pure graphene oxide. The bands at 3419, 1720, 1578, 1287, 1177, and 1069  $\text{cm}^{-1}$  correspond to carboxylic acids, carbonyls, aromatic double bonds, ether groups, and C-O stretching vibrations, respectively [47]. The bands at 845 and 875  $\text{cm}^{-1}$  can be assigned to epoxide vibrations. The band at 568  $\text{cm}^{-1}$  can be also attributed to CH bending vibrations.

**Fig. 1b** shows the FTIR spectrum of Diethylenetriamine-functionalized graphene oxide (GO@DETA). The strong broadband at 3438  $\text{cm}^{-1}$  corresponds to OH and NH stretching vibrations. The bands appeared at 2856 and 2925  $\text{cm}^{-1}$  can be related to diethylenetriamine CH stretching vibrations. Also, the band corresponding to C=C emerged at 1636  $\text{cm}^{-1}$ . Stretching vibration of the carbonyl amide group on the graphene oxide surface (C=O) can be observed at 1695  $\text{cm}^{-1}$ . The strong vibration bands of C-O also appeared at 1083 and 1098  $\text{cm}^{-1}$ . Bending vibrations of aliphatic diethylenetriamine N-H bonds or out-plane bending of C=C aromatic ring vibrations in GO@DETA can also be detected at 612  $\text{cm}^{-1}$ . Compared to graphene oxide, this band was stronger in GO@DETA. In comparison with graphene oxide, CH stretching bands appeared at 2856 and 2925  $\text{cm}^{-1}$  in the case of GO@DETA confirming the diethylenetriamine-functionalization of graphene oxide. Moreover, the C=C stretching band got stronger in GO@DETA reflecting the formation of benzene rings on the skeleton of graphene oxide. Carbonyl group (C=O) at the graphene oxide spectrum appeared at 1720  $\text{cm}^{-1}$ , while in the case of GO@DETA, this band emerged at 1697  $\text{cm}^{-1}$ . This shift indicates the formation of amide functional groups.

**Fig. 1b** shows the FTIR spectrum of the PE@GO-DETA-Thiazole-TFA composite. Bands at 2850 and 2951  $\text{cm}^{-1}$  can be mainly attributed to the polyethylene CH stretching vibrations [48] as well as diethylenetriamine and hexamethylenediamine CH vibrations. The bands at 1677 to 1697  $\text{cm}^{-1}$  can be assigned to amide carbonyl groups in graphene oxide and urea carbonyl groups [49] and trifluoroacetate carbonyl groups [50]. A strong broad band at 3388  $\text{cm}^{-1}$  can be ascribed to amide and urea NH, OH on the graphene oxide surface, and carboxylic acid OH on the

graphene oxide. C=C stretching vibration band of graphene oxide appeared at 1626  $\text{cm}^{-1}$ . The bands at 1575, 1513, 1467, and 1405  $\text{cm}^{-1}$  are related to polyethylene CH vibrations [47]. C=C vibrations of thiazole group emerged at 1575  $\text{cm}^{-1}$  [51, 52]. The band appearing at 1253  $\text{cm}^{-1}$  corresponds to thiazole vibrations. While the band at 1203  $\text{cm}^{-1}$  can be assigned to  $\text{CF}_3\text{COO}^-$  vibrations. C-O and O-H vibrations of graphene oxide can be found at 1042 and 1085  $\text{cm}^{-1}$ . The band at 880  $\text{cm}^{-1}$  corresponds to the out- plane bending vibrations of C=C in the thiazole group [51, 52]. The band at 721  $\text{cm}^{-1}$  corresponds to polyethylene [48], thiazole C-H vibrations, and  $\text{CF}_3\text{COO}^-$  C-F vibrations. The emergence of new bands corresponding to polyethylene, thiazole, hexamethylene diamine, and  $\text{CF}_3\text{COO}^-$  (compared to the FTIR spectrum of GO and GO@DETA) in the spectrum of catalyst confirm the presence of these constituents in the structure of PE@GO-DETA-Thiazole-TFA composite.

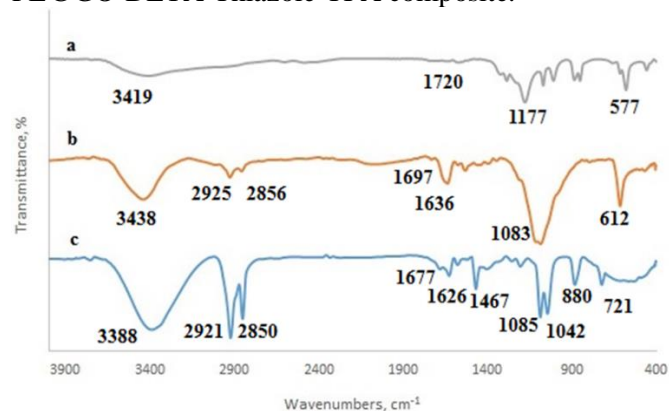


**Fig. 1.** FT-IR spectra of GO (a), GO@DETA (b) and PE@GO-DETA-Thiazole-TFA composite (c).

**3.4. XRD spectra**

**Fig. 2** shows the XRD pattern of GO, GO@DETA, and trifluoroacetate-bonded polyethylene graphene oxide composite. The peak at  $2\theta = 9.55^\circ$  corresponds to graphene oxide [53] while the broad peak at  $2\theta = 20.25^\circ$  indicates the presence of reduced graphene oxide (at small amounts) in the sample (**Fig. 2a**). This reduced graphene oxide could be formed through ultrasonic bath exfoliation of graphene oxide during the purification process for the preparation of graphene oxide nanoplatelets. XRD pattern of GO@DETA is depicted in **Fig. 2b**. The peak corresponding to graphene oxide at  $2\theta = 9.55^\circ$  disappeared and new peaks emerged at  $2\theta = 15-32^\circ$ , indicating the products crystallinity with various d-spacing, probably due to diethylenetriamine-functionalization of graphene oxide (**Fig. 2c**). XRD pattern of composite shows two strong and sharp peaks of polyethylene at  $2\theta = 22^\circ$  and  $24^\circ$  [54] and a broad

amorphous pattern of GO@DETA in  $2\theta = 17-26^\circ$ . In conclusion, the catalyst includes polyethylene and functionalized graphene oxide which is in agreement with FTIR spectra (Fig. 1).

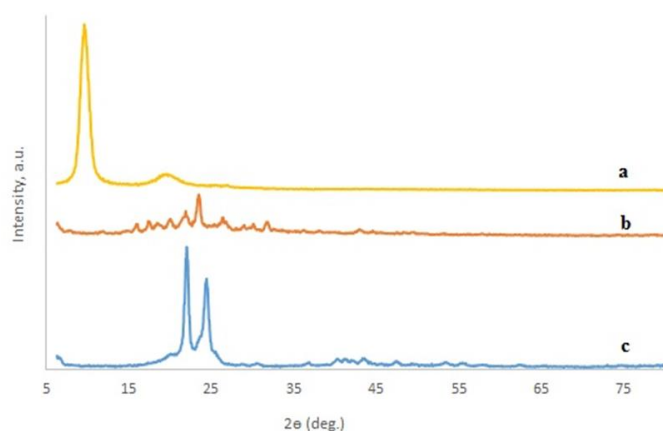


**Fig. 2.** XRD spectra of GO (a), GO@DETA (b) and PE@GO-DETA-Thiazole-TFA composite (c).

### 3.5. FESEM images and EDS analysis

FESEM image of GO@DETA shows the crumbled and planar graphene oxide sheets due to diethylenetriamine-functionalization of graphene oxide (Fig. 3a, b). After sonication and preparation of trifluoroacetate-bonded polyethylene graphene oxide composite, the composite (including exfoliated graphene sheets and polyethylene) was obtained (Fig. 3c, d). As illustrated in Fig. 4, energy dispersive x-ray spectroscopy (EDS) analysis approved the presence of diethylenetriamine on the surface of graphene oxide. Three elements (C, N, and O) were present in EDS results whose percentages are reported in Table (Fig.4). Fig. 5 exhibits the EDS analysis of trifluoroacetate-bonded polyethylene graphene oxide composite and shows the presence of C, N, O, F, and S on the surface. The percentages of the mentioned elements are reported in Table (Fig. 5). In agreements with FTIR and XRD results, EDS confirms the structure of the composite and the presence of polyethylene, graphene oxide, thiazole, and trifluoroacetate moieties.

### 3.6. TGA analysis

The thermal stability of the trifluoroacetate-bonded polyethylene graphene oxide composite was investigated by TGA analysis as presented in Fig. 6. The first degradation occurred at 90-125 °C due to the presence of trapped solvents and  $\text{CF}_3\text{COO}^-$  in the structure. The main structure of the polymer remained stable from 125 °C to 450 °C. The final degradation took place at 450-500 °C [55]. Accordingly, the presence of functional groups reduced the thermal stability at ~100 °C.

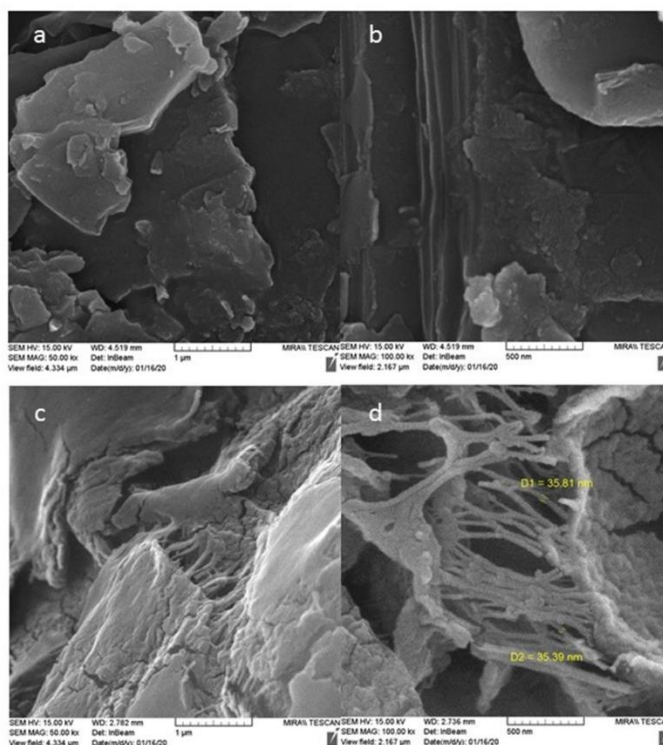


**Fig. 3.** FESEM images of GO@DETA (a, b) and PE@GO-DETA-Thiazole-TFA composite (c, d).

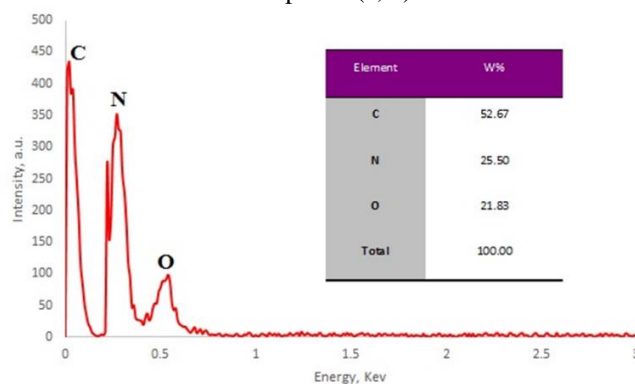


**Fig. 4.** EDS analysis of GO@DETA.

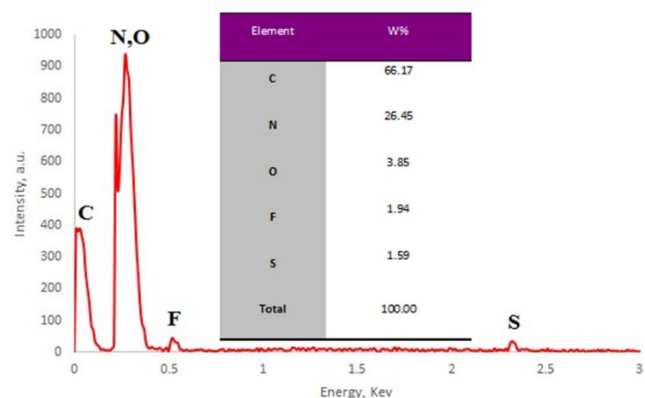


**Fig. 5.** EDS analysis of PE@GO-DETA-Thiazole-TFA composite.

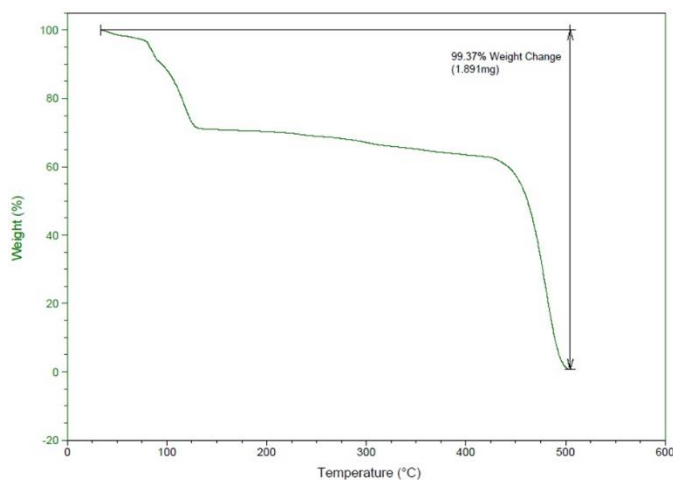
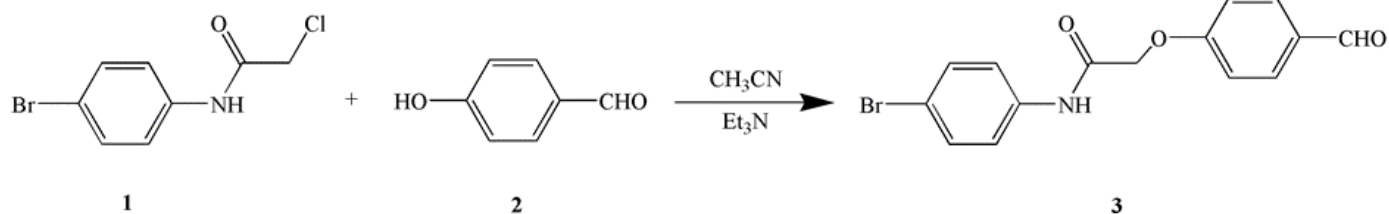


**Fig. 6.** TGA analysis of PE@GO-DETA-Thiazole-TFA composite.

### 3.7. Synthesis of **3**

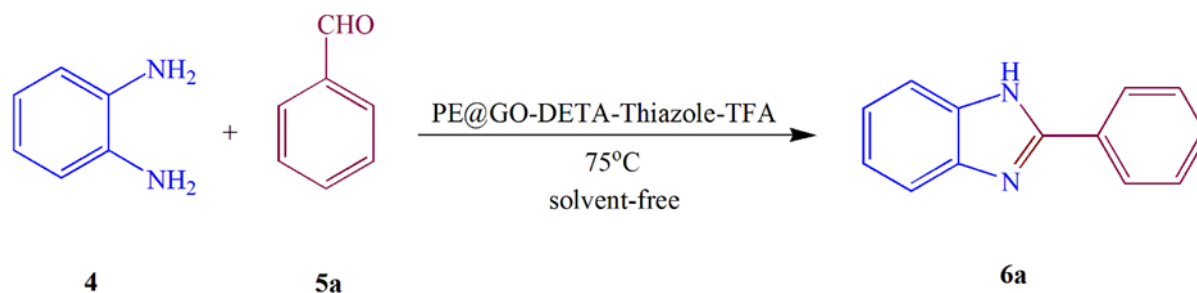


**Scheme 4.** Synthesis of **3**.

### 3.8. Synthesis of benzimidazoles using trifluoroacetate-bonded polyethylene graphene oxide composite

To examine the efficiency of the trifluoroacetate-bonded polyethylene graphene oxide composite in organic reactions, the synthesis of benzimidazoles was explored. According to the model reaction (**Scheme 5**), benzimidazole was synthesized using 1,2-phenylenediamine, benzaldehyde, and composite under various conditions (different composite loadings, temperatures, and durations with/without solvent) (**Table 1**). Thin-layer chromatography (TLC) was also employed to monitor the progress of the reaction and determine the yields of isolates. The catalyst-free

reaction shows slow progress in 6h and only 11% of the product was obtained by refluxing with ethanol. Therefore, the catalyst should be used for the synthesis. Consequently, 0.02g of the composite was added to methanol and ethanol solvents for 1h under reflux condition, giving rise to 80 and 62% product yields, respectively. Then, the solvent-free condition was implemented using 0.01 g of composite at 70 °C for 1h, giving rise to the 75% yield. Similarly, the composite content, temperature, and duration were changed to optimize the condition as reported in entry 11 of **Table 1**. In conclusion, the optimum condition involves using 0.02g composite, at 75°C for 60 min under solvent-free conditions.



**Scheme 5.** Model reaction for the synthesis of **6a**.

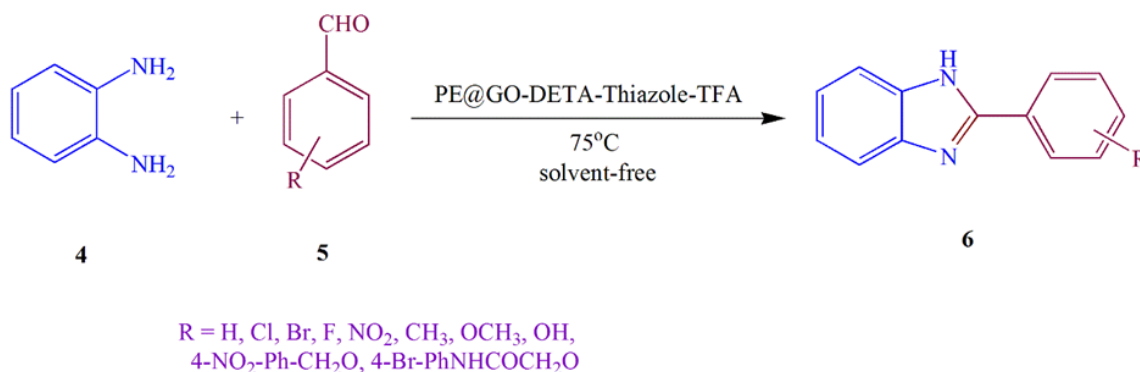
**Table 1.** Optimization of the reaction conditions for **6a** (benzimidazole)

Entry	Solvent	Catalyst (g)	Temperature (°C)	Time/h	Yield (%) <sup>a</sup>
1	EtOH	-	Reflux	6.0	11
2	EtOH	0.02	Reflux	2.0	80
2	MeOH	0.02	Reflux	2.0	62
3	Solvent-free	0.01	70	2.0	75
4	Solvent-free	0.01	80	2.0	78
5	Solvent-free	0.01	80	2.5	84
6	Solvent-free	0.01	90	2.0	81
7	Solvent-free	0.02	60	2.0	71
8	Solvent-free	0.02	70	2.0	94
9	Solvent-free	0.02	80	2.0	96
10	Solvent-free	0.02	90	2.0	97
11	Solvent-free	0.02	75	1.0	96
12	Solvent-free	0.02	75	0.5	83
13	Solvent-free	0.03	75	1.0	97
14	Solvent-free	0.04	75	1.0	97

a) Isolated yield

To explore the composite scope, various aldehydes with miscellaneous substituents were applied to prepare benzimidazoles (**Scheme 6**). According to **Table 2**, good to excellent yields could be attained depending on the substituents. The nature of the substituents influenced the time of reaction where the electron-withdrawing ones took shorter times to complete. Based on the mechanism of reaction, protonation of aldehyde

along with electron-withdrawing substituents at the first step increased the nucleophilicity of the carbonyl group; then incremented the reaction rate. This effect will be inverse for electron-donating groups and the protonation process in the first step will occur at lower rates, then declined the yields and reaction rates. However, ortho-substituted aldehyde with electron-withdrawing and electron-donating substituents took longer reaction times due to the steric hindrance.

**Scheme 6.** Reaction route for the synthesis of benzimidazoles.

**Table 2.** Synthesis of different benzimidazoles using trifluoroacetate-bonded polyethylene graphene oxide composite

Entry	R	Product	Time/Min.	Yield (%) <sup>a</sup>	MP/°C	
					Found	Reported
1	H	6a	60	96	291-292	292-293[56]
2	4-Me	6b	60	95	276-277	275-276[57]
3	4-MeO	6c	60	95	223-224	224-225[56]
4	4-(CH <sub>3</sub> ) <sub>2</sub> N	6d	60	90	293-294	292-294[57]
5	2-OH	6e	70	89	236-237	237-238[57]
6	4-Cl	6f	60	97	287-288	289-291[56]
7	4-Br	6g	60	95	299-300	300-301[58]
8	4-OH	6h	80	87	253-254	254-256[59]
9	2,4-di-Cl	6i	80	88	228-229	230-232[60]
10	3-O <sub>2</sub> N	6k	60	90	199-200	200-202[61]
11	4-O <sub>2</sub> N	6l	60	94	309-310	308-310[62]
12	4-NO <sub>2</sub> -Ph-CH <sub>2</sub> O[63]	6m	90	94	156-158	156-157[64]
13	4-BrPhNHCOCH <sub>2</sub> O	6n	90	92	173-174	-

a) Isolated yield.

<sup>1</sup>H NMR and <sup>13</sup>C NMR spectroscopy were utilized to confirm the structure of **6m**. Based on <sup>1</sup>H NMR results, two methylene protons can be observed as singlet in 5.25 ppm. Two protons appeared in the range of 6.97-7.03 ppm as multiplet. In 7.28 ppm with  $J = 12$  Hz, one aromatic proton was determined as doublet. One aromatic proton as doublet was also recorded in 7.36 ppm with  $J = 12$  Hz. In 7.51 ppm with  $J = 12$  Hz, one aromatic proton was detected as doublet.

Two aromatic protons could be detected in the range of 7.69-7.73 ppm as multiplet. Also, two protons were detected in the range of 7.77-7.81 ppm as multiplet. In 8.19 ppm with  $J = 8$  Hz, one doublet proton was detected. Three protons could be detected in the range of 8.26-8.34 ppm as a multiplet. <sup>13</sup>C NMR spectrum showed one aliphatic and 12 aromatic carbons. Thus, <sup>1</sup>H NMR and <sup>13</sup>C NMR results confirmed the structure of **6m**. Moreover, the mass spectrum represented the molecular mass of **6m** at  $m/z$  of 345 confirming the molecular mass.

(**6n**) was further studied by <sup>1</sup>H NMR and <sup>13</sup>C NMR spectroscopy. Based on the <sup>1</sup>H NMR results, two singlet

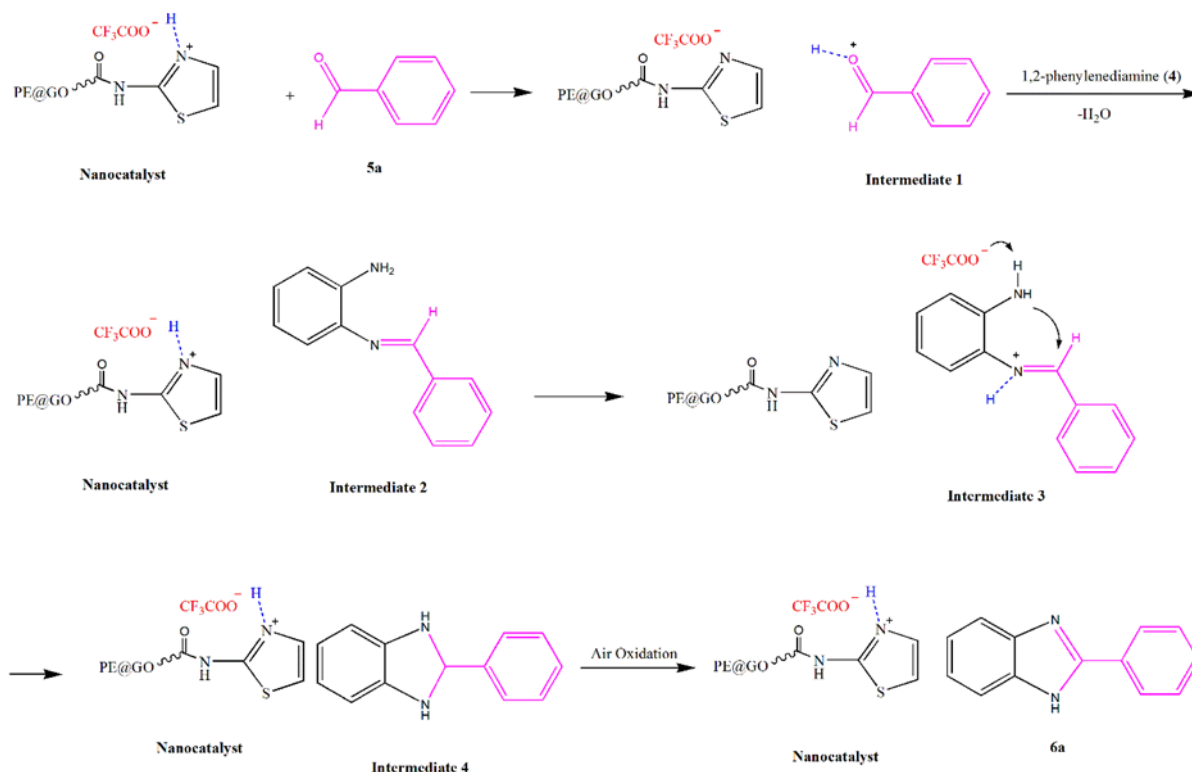
methylene protons appeared in 4.92 ppm. In the range of 7.12-7.79 ppm, 11 aromatic and NH protons emerged as multiplet. In 8.19 ppm with  $J = 9$  Hz, two doublet aromatic protons were detected. One singlet NH proton was also found at 10.38 ppm. <sup>13</sup>C NMR spectrum showed one aliphatic, 18 aromatics, and one carbonyl carbons. Thus, <sup>1</sup>H NMR and <sup>13</sup>C NMR confirm the structure of **6n**. The mass spectrum showed a mass of **6n** at  $m/z$  of 422 and confirming its molecular mass.

### 3.9. Composite (catalyst) reusability and activity

The reusability of the trifluoroacetate-bonded polyethylene graphene oxide composite was also assessed. For this purpose, after completion of **6a** synthesis, the composite was recovered by adding hot ethanol to the reaction mixture followed by filtration. The recovered composite on the filter paper was dried at room temperature and reused in another reaction. This process was repeated for five cycles. According to the results, the composite retained its activity for five cycles with no significant decline in its activity (**Fig. 7**).

### 3.10. Reaction mechanism

The proposed reaction mechanism is presented in **Scheme 7**. At first, the aldehyde functional groups were activated by the composite (intermediate 1) to increase the electrophilic properties of the carbonyls and attack of 1,2-phenylenediamine  $\text{-NH}_2$ , giving rise to imine formation (intermediate 2). In the next step, intermediate 2 was protonated through the nitrogen of imine (intermediate 3); second  $\text{-NH}_2$  of 1,2-phenylenediamine attacked the imine bond to form dihydroimidazole (intermediate 4). Ultimately, 2-aryl-1H-benzimidazole (**6a**) was obtained by air oxidation of dihydroimidazole and aromatic recovery.



**Scheme 7.** Proposed mechanism of 2-aryl-1H-benzimidazole (**6a**) formation in the presence of PE@GO-DETA-Thiazole-TFA composite.

### 3.11. Advantages over other catalytic systems

The synthesis of 2-aryl-1H-benzimidazole has been extensively studied utilizing diverse catalysts. **Table 3** compares the present trifluoroacetate-bonded polyethylene graphene oxide composite (catalyst) with those previously-reported in the synthesis of benzimidazoles. As can be seen, these catalysts suffer from some disadvantages including toxic nature, tedious workup and the use of toxic solvents as reaction medium and workup. Polyethylene and graphene are inexpensive materials. Graphene is nontoxic and the waste polyethylene or postconsumer polyethylene can be used for the preparation of catalysts which can help in protecting the environment [65]. Thus, this type of

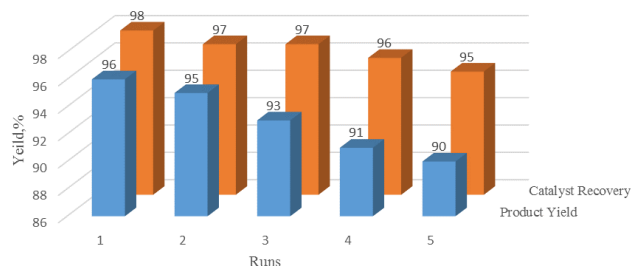


**Fig. 7.** Composite (catalyst) recovery and product yields (**6a**) for five runs.

catalyst design can help in protecting the environment by removing the toxic waste. This composite (catalyst) system also exhibited significant characteristics of green catalytic systems such as activity, environmental-friendliness, cost-effectiveness, recyclability, and ease of separation. According to the TGA analysis, the trifluoroacetate-bonded polyethylene graphene oxide composite was decomposed at temperatures above  $450^\circ\text{C}$ . After using the composite, its reminders can be transformed into other organic compounds through pyrolysis process.

## 4. Conclusions

An efficient novel trifluoroacetate-bonded polyethylene graphene oxide composite was designed and prepared

based on the polyethylene, diethylenetriamine-functionalized graphene oxide, and trifluoroacetic acid. FTIR, XRD, FESEM, EDS, and TGA techniques confirmed the structure of the composite. Benzimidazole can be successfully prepared in the presence of the proposed catalyst through a solvent-free process. The recovery and reusability of the composite for five runs showed no considerable loss of product yield. The proposed composite (catalyst) had several

superiorities over the conventional catalysts in the synthesis of benzimidazoles. The process for the preparation of benzimidazoles has also some advantages including solvent-free and moderate conditions, facile workup, cost-effectiveness, and the use of nonmetal catalysts. Polyethylene is a widely employed and accessible industrial polymer. Thus, post-consumer polyethylene can be used for the preparation of catalysts which can be helpful in environmental protection.

**Table 3.** Comparison of the synthesis of 2-aryl-1H-benzimidazole (**6a**) catalyzed by trifluoroacetate-bonded polyethylene graphene oxide composite (catalyst) with those obtained by the other catalyst<sup>a</sup>

Entry	Catalyst	Solvent	Temperature, (°C)	Time (Min.)	Yield <sup>b</sup> (%) <sup>Ref.</sup>
1	Ce(NO <sub>3</sub> ) <sub>3</sub> .6H <sub>2</sub> O (30 mol%)	DMF	80	120	93[66]
2	Pt/TiO <sub>2</sub> (1 mol%)	Mesitylene	RT	60	78[67]
3	Co(OH) <sub>2</sub> (10 mol%)	EtOH	RT	240	96[21]
4	PhSiH <sub>3</sub> (4eq)	DMF	120	120	95[68]
5	CuI Nps (10 mol%)	CH <sub>3</sub> CN/O <sub>2</sub>	RT	60	96[69]
6	CuFe <sub>2</sub> O <sub>4</sub> NPs (20 mol%)	Toluene/O <sub>2</sub>	110	1440	89[70]
7	Silica Sulfuric acid (10 mg)	CH <sub>2</sub> Cl <sub>2</sub> /O <sub>2</sub>	RT	60	82[60]
8	This catalyst (20 mg)	Solvent-free	75	60	96, This work

a)The reactions were carried out by the condensation of 1,2-phenylenediamine with benzaldehyde. b) Isolated yield

## Acknowledgements

The authors would like to appreciate the Payame Noor University (PNU) Research Council for supporting this research study.

## Conflict of Interest

The authors declare no conflict of interest.

## References

- [1] R. A. Sheldon, *Curr. Opin. Green Sustain. Chem.* 18 (2019) 13-19.
- [2] N. Jiao, S. S. Stahl, eds., *Green Oxidation in Organic Synthesis*. John Wiley & Sons, (2019), Incorporated.
- [3] M. Burgman, M. Tennant, N. Voulvoulis, K. Makuch, K. Madani, *Curr. Opin. Green Sustain. Chem.* 13 (2018) 130-136.
- [4] M. Hu, Z. Yao, X. Wang, *Ind. Eng. Chem. Res.* 56 (2017) 3477-3502.
- [5] B. Qiu, M. Xing, Zhang, *J. Chem. Soc. Rev.* 47 (2018) 2165-2216.
- [6] M. Hussain, R. A. Naqvi, N. Abbas, S. M. Khan, S. Nawaz, A. Hussain, N. Zahra, M. W. Khalid, *Polymers* 12 (2020) 323.
- [7] T. K. Glaser, O. Plohl, A. Vesel, U. Ajdnik, N. P. Ulrih, M. K. Hrnčič, U. Bren, L. Fras Zemljčič, *Materials* 12 (2019) 2118.
- [8] A. M. Ganie, A. M. Dar, F. A. Khan, B. A. Dar, *Mini-Rev. Med. Chem.* 19 (2019) 1292-1297.
- [9] S. Tahlan, S. Kumar, B. Narasimhan, *BMC Chem.* 13 (2019) 101.
- [10] B. Maiti, K. Chanda, *RSC Adv.* 6 (2016) 50384-50413.
- [11] M. Hamiduzzaman, S. J. Mannan, A. Dey, S. M. Abdur Rahman, *Der Pharm. Lett.* 6 (2014) 47-53.
- [12] J. Ramprasad, N. Nayak, U. Dalimba, P. Yogeewari, D. Sriram, S. K. Peethambar, R. Achur, H. S. S. Kumar, *Eur. J. Med. Chem.* 95 (2015) 49-63.
- [13] T. Pan, X. He, B. Chen, H. Chen, G. Geng, H. Luo, H. Zhang, C. Bai, *Eur. J. Med. Chem.* 95 (2015) 500-513.
- [14] A. P. Nikalje, M. Ghodke, *World J. Pharm. Pharm. Sci.* 3 (2013) 1311-1322.
- [15] N. K. Prashant, K. R. Kumar, *Inter. J. Pharm. Tech. Res.* 8 (2015) 60-63.
- [16] H. Panwar, R. Dubey, N. Chaudhary, T. Ram, *Der Pharm. Chem.* 5 (2013) 192-200.
- [17] A. Patil, S. Ganguly, S. Surana, *Rasayan J. Chem.* 1 (2008) 447-460.
- [18] Y. T. Wang, Y. J. Qin, N. Yang, Y. L. Zhang, C. H. Liu, H. L. Zhu, *Eur. J. Med. Chem.* 99 (2015) 125-137.
- [19] A. Kulshreshtha, *Inter. J. Res-Granthaalayah* 3 (2015) 1-7.
- [20] S. Singhal, P. Khanna, S. S. Panda, L. Khanna, *J. Heterocycl. Chem.* 56 (2019) 2702-2729.
- [21] M. A. Chari, D. Shobha, T. Sasaki, *Tetrahedron Lett.* 52 (2011) 5575-5580.
- [22] R. Trivedi, S. K. De, R. A. Gibbs, *J. Mol. Catal. A-Chem.* 245 (2006) 8-11.
- [23] C. Stevenson, R.J.H. Davies, *Chem. Res. Toxicol.* 12 (1999) 38-45.
- [24] A. Saberi, *Iran. J. Sci. Technol.* 39 (2015) 7-10.

- [25] F. F. Bamoharram, M. M. Heravi, M. Hosseini, K. Bakhtiari, Iran. J. Org. Chem. 1 (2008) 25-27.
- [26] B. G. Mohamed, A.-A. M. Abdel-Alim, M.A. Hussein, Acta Pharm. 56 (2006) 31-48.
- [27] G. Mariappan, R. Hazarika, F. Alam, R. Karki, U. Patangia, S. Nath, Arab. J. Chem. 8 (2015) 715-719.
- [28] A. Patil, S. Ganguly, S. Surana, Rasayan J. Chem. 1 (2008) 447-460.
- [29] S. Rithe, R. Jagtap, S. Ubarhande, Rasayan J. Chem. 8 (2015) 213-217.
- [30] Z. H. Zhang, T. S. Li, J. J. Li, Monatsh. Chem. 138 (2007) 89-94.
- [31] H. Sharma, N. Kaur, N. Singh, D. O. Jang, Green Chem. 17 (2015) 4263-4270.
- [32] A. V. Narsaiah, A. R. Reddy, J. S. Yadav, Synth. Commun. 41 (2010) 262-267.
- [33] M. Lei, L. Ma, L. Hu, Synth. Commun. 42 (2012) 2981-2993.
- [34] G. Navarrete-Vázquez, H. Moreno-Díaz, S. Estrada-Soto, M. Torres-Piedra, I. León-Rivera, H. Tlahuext, O. Muñoz-Muñiz, H. Torres-Gómez, Synth. Commun. 37 (2007) 2815-2825.
- [35] H. Sharghi, O. Asemani, R. Khalifeh, Synth. Commun. 38 (2008) 1128-1136.
- [36] V. K. Tandon, M. Kumar, Tetrahedron Lett. 45 (2004) 4185-4187.
- [37] A. Sajjadi, R. Mohammadi, J. Med. Chem. Sci. 2 (2019) 55-58.
- [38] K. B. Dhopte, R. S. Zambare, A. V. Patwardhan, P. R. Nemade, RSC Adv. 6 (2016) 8164-8172.
- [39] P. K. Dhiman, R. K. Mahajan, I. Kaur, J. Appl. Polym. Sci. 121 (2011) 2584-2590.
- [40] M. Pervaiz, P. Oakley, M. Sain, Mater. Sci. Appl. 5 (2014) 845-856.
- [41] M. Y. Abdelaal, E. H. Elmoosalamy, S. O. Bahaffi, Am. J. Polym. Sci. 2 (2012) 102-108.
- [42] W. S. Hummers, R. E. Offeman, J. Am. Chem. Soc. 80 (1958) 1339.
- [43] R. Muzyka, M. Kwoka, Ł. Smędowski, N. Díez, G. Gryglewicz, New Carbon Mater. 32 (2017) 15-20.
- [44] M. Saeedi, F. Goli, M. Mahdavi, G. Dehghan, M.A. Faramarzi, A. Foroumadi, A. Shafiee, Iran J. Pharm. Res. 13 (2014) 881-892.
- [45] J. R. Araujo, M. R. Vallim, M. A. S. Spinacé, M. A. De Paoli, J. Appl. Polym. Sci. 110 (2008) 1310-1317.
- [46] J. S. Park, Y. M. Lim, Y. C. Nho, Materials 9 (2016) 13.
- [47] A. Alizadeh, G. Abdi, M.M. Khodaei, M. Ashok kumar, J. Amirian, RSC Adv. 7 (2017) 14876-14887.
- [48] J. X. Wong, S. N. Gan, M. J. Aishah, Sains Malays. 40 (2011) 771-779.
- [49] I. Yilgor, E. Yilgor, I. G. Guler, T. C. Ward, G. L. Wilkes, Polymer 47 (2006) 4105-4114.
- [50] M. Grundwald-Wyspianska, M. Szafran, J. Mol. Liq. 33 (1987) 245-254.
- [51] H. N. Karade, B. N. Acharya, M. Sathe, M. P. Kaushik, Med. Chem. Res. 17 (2008) 19-29.
- [52] N. Singh, U. S. Sharma, N. Sutar, S. Kumar, U. K. Sharma, J. Chem. Pharm. Res. 2 (2010) 691-698.
- [53] S. A. Soomro, I. H. Gul, H. Naseer, S. Marwat, M. Mujahid, Curr. Nanosci. 15 (2019) 420-429.
- [54] G. Tadayyon, S. M. Zebarjad, S. A. Sajjadi, J. Thermoplast. Compos. Mater. 25 (2012) 479-490.
- [55] R. Arrigo, P. Jagdale, M. Bartoli, A. Tagliaferro, G. Malucelli, Polymers 11 (2019) 1336.
- [56] J. Lu, B. Yang, Y. Bai, Synth. Commun. 32 (2002) 3703-3709.
- [57] B. Eren, Y. Bekdemir, Quim. Nova 37 (2014) 643-647.
- [58] D. Yang, X. Zhu, W. Wei, N. Sun, L. Yuan, M. Jiang, J. You, H. Wang, RSC Adv. 4 (2014) 17832-17839.
- [59] G. Navarrete-Vázquez, H. Moreno-Díaz, S. Estrada-Soto, M. Torres-Piedra, I. León-Rivera, H. Tlahuext, O. Muñoz-Muñiz, H. Torres-Gómez, Synth. Commun. 37 (2007) 2815-2825.
- [60] B. Das, B. S. Kanth, K. R. Reddy, A. S. Kumar, J. Heterocycl. Chem. 45 (2008) 1499-1502.
- [61] M. R. DeLuca, S. M. Kerwin, Tetrahedron 53 (1997) 457.
- [62] A. Ben-Alloum, K. Bougrin, M. Soufiaoui, Tetrahedron Lett. 44 (2003) 5935.
- [63] E. Rostami, S. Hamidi Zare, ChemistrySelect 4 (2019) 13295-13303.
- [64] R. Afsharpour, S. Zanganeh, S. Kamantorki, F. Fakhraei, E. Rostami, Asian J. Nanosci. Mater. 3 (2020) 148-156.
- [65] M. R. Nabid, Y. Bide, M. Jafari, Polym. Degrad. Stabil. 169 (2019) 108962.
- [66] G. M. Martins, T. Puccinelli, R. A. Gariani, F. R. Xavier, C. C. Silveira, S. R. Mendes, Tetrahedron Lett. 58 (2017) 1969-1972.
- [67] C. Chaudhari, S. M. A. Hakim Siddiki K. Shimizu, Tetrahedron Lett. 56 (2015) 4885-4888.
- [68] J. Zhu, Z. Zhang, C. Miao, W. Liu, W. Sun, Tetrahedron 73 (2017) 3458-3462.
- [69] P. Linga Reddy, R. Arundhathi, M. Tripathi, D. S. Rawat, RSC Adv. 6 (2016) 53596-53601.
- [70] D. Yang, X. Zhu, W. Wei, N. Sun, L. Yuan, M. Jiang, J. You, H. Wang, RSC Adv. 4 (2014) 17832-17839.